

Robust Perfect Adaptation of Reaction Fluxes Ensured by Network Topology

Yuji Hirono,^{1,2,3,*} Hyukpyo Hong,^{4,5,†} and Jae Kyoung Kim^{4,5,‡}

¹Asia Pacific Center for Theoretical Physics, Pohang 37673, Republic of Korea

²Department of Physics, POSTECH, Pohang 37673, Republic of Korea

³RIKEN iTHEMS, RIKEN, Wako 351-0198, Japan

⁴Department of Mathematical Sciences, Korea Advanced Institute of Science and Technology, Daejeon 34141, Republic of Korea

⁵Biomedical Mathematics Group, Pioneer Research Center for Mathematical and Computational Sciences,

Institute for Basic Science, Daejeon 34126, Republic of Korea

(Dated: February 3, 2023)

Maintaining stability in an uncertain environment is essential for proper functioning of living systems. Robust perfect adaptation (RPA) is a property of a system that generates an output at a fixed level even after fluctuations in input stimulus without fine-tuning parameters, and it is important to understand how this feature is implemented through biochemical networks. The existing literature has mainly focused on RPA of the concentration of a chosen chemical species, and no generic analysis has been made on RPA of reaction fluxes, that play an equally important role. Here, we identify structural conditions on reaction networks under which all the reaction fluxes exhibit RPA against the perturbation of the parameters inside a subnetwork. Based on this understanding, we give a recipe for obtaining a simpler reaction network, from which we can fully recover the steady-state reaction fluxes of the original system. This helps us identify key parameters that determine the fluxes and study the properties of complex reaction networks using a smaller one without losing any information about steady-state reaction fluxes.

Introduction.—How to keep a stable status in a changing environment is a vital issue for biological systems [1, 2]. One strategy that living cells adopt for maintaining stability is robust perfect adaptation (RPA) [3–7], which is a property of a system that maintains the levels of certain quantities by counteracting the effect of disturbances inside biochemical reaction networks [8–10]. From a control-theoretical viewpoint, RPA can be achieved through integral feedback control [7, 11, 12], and there have been studies on how to implement this within biochemical reaction networks for a chosen set-point concentration [13–15]. As an alternative perspective, a topological criterion is developed to identify subnetworks whose parameters are irrelevant to the steady-state properties of the rest of the network [16–18] (see also Refs. [19–21]). In other words, the rest of the network exhibits RPA with respect to the perturbation of reaction parameters inside subnetworks that satisfy certain topological conditions.

So far, the study of RPA has focused mainly on the adaptation of the concentration of a fixed chemical species. However, in many biological contexts, reaction fluxes play an equally important role. For example, they are used as a measure of biomass production or cell growth [22]. Despite this, a comprehensive analysis of RPA of reaction fluxes in relation to the underlying network structure has so far been elusive. In this Letter, we uncover the topological criterion for identifying the parameters to which *all* the reaction fluxes exhibit RPA for generic chemical reaction systems. We further show that the steady-state reaction fluxes can be reconstructed from those of a simpler reduced system, which is easier to analyze. Namely, the reduced system is the smallest faithful representation of the original system in the sense that the steady-state reaction fluxes can be fully re-

constructed. We will demonstrate the method with simple hypothetical examples as well as a realistic network of the metabolic pathways of *Escherichia coli* (*E. coli*). Our finding allows us to identify the parameters that are relevant in determining the reaction fluxes in a possibly complex reaction network and helps us to understand the behavior of the system. As an advantage of the present method, we stress that we do not assume any particular reaction kinetics; hence, the results are broadly applicable to generic reaction systems.

Chemical reaction systems.—We consider a deterministic chemical reaction system based on a reaction network $\Gamma = (V, E)$, where V and E are sets of chemical species and reactions, respectively. Reaction $e_A \in E$ can be specified in the form



where $v_i \in V$, and y_{iA} and \bar{y}_{iA} are stoichiometric coefficients of species v_i . We denote the stoichiometric matrix by S , whose components are given by $S_{iA} := \bar{y}_{iA} - y_{iA}$. Using S , we can write down the rate equations that describe the time evolution of chemical concentrations:

$$\frac{d}{dt} \mathbf{x}(t) = S \mathbf{r}, \quad (2)$$

where x_i is the concentration of v_i and r_A is the reaction rate (i.e., fluxes) of reaction e_A . To solve the rate equations, we need to express the reaction fluxes, r_A , as functions of reactant concentrations, \mathbf{x} , and parameters, k_A , and this choice is called *kinetics*, i.e., $r_A = r_A(\mathbf{x}; k_A)$.

We consider a situation where the system reaches an asymptotically-stable steady state in the long-time limit,

and examine how the system responds to changes in parameters. The steady-state solution can be obtained by solving $S\mathbf{r} = \mathbf{0}$. When the stoichiometric matrix has a nontrivial cokernel (left null space), the system has conserved charges, and we can specify their values to obtain the steady-state solution [23]: if we pick a basis $\{\mathbf{d}^{(\bar{\alpha})}\}_{\bar{\alpha}}$ of coker S , they can be fixed by

$$\ell^{\bar{\alpha}} = \mathbf{d}^{(\bar{\alpha})} \cdot \mathbf{x}, \quad (3)$$

where $\ell^{\bar{\alpha}} \in \mathbb{R}$ specifies the value of the conserved charge $\mathbf{d}^{(\bar{\alpha})} \cdot \mathbf{x}$.

Robust perfect adaptation of reaction fluxes.—We find that there is a simple topological criterion for identifying the parameters to which all the reaction fluxes exhibit RPA. The topological condition is expressed by an index, which we will define below.

Let us choose a subnetwork $\gamma = (V_\gamma, E_\gamma)$ of $\Gamma = (V, E)$, i.e., $V_\gamma \subset V$ and $E_\gamma \subset E$. If E_γ includes all the reactions whose reactants are in V_γ , we call the subnetwork to be *output-complete*. For an output-complete subnetwork γ , we introduce the *flux influence index*, which is an integer given by

$$\lambda_f(\gamma) := -|V_\gamma| + |E_\gamma| + |P_\gamma^0(\text{coker } S)|. \quad (4)$$

The first two terms are the number of chemical species and reaction in the subnetwork, respectively, and the last term is the dimension of projected coker S to the species in γ :

$$P_\gamma^0(\text{coker } S) := \{P_\gamma^0 \mathbf{d} \mid \mathbf{d} \in \text{coker } S\}, \quad (5)$$

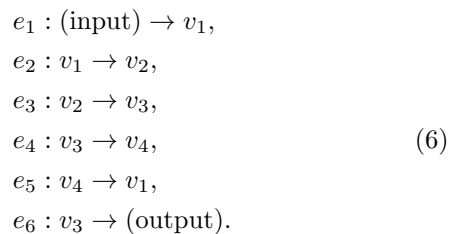
where P_γ^0 is the projection matrix to the species in γ . Intuitively, $|P_\gamma^0(\text{coker } S)|$ counts the number of conserved charges that include the species inside γ . The flux influence index $\lambda_f(\gamma)$ can be used to identify irrelevant subsystems for determining the steady-state reaction fluxes as follows¹.

Theorem 1 (RPA of reaction fluxes). Let $\gamma \subset \Gamma$ be an output-complete subnetwork of a chemical reaction network Γ . When γ satisfies $\lambda_f(\gamma) = 0$, steady-state reaction fluxes of Γ do not change under the variation of rate parameters of the reactions inside γ and the values of conserved charges that have nonzero support in γ . Namely, the steady-state reaction flux \bar{r}_A of *any* reaction in Γ , $e_A \in E$, satisfies $\frac{\partial}{\partial k_{B^*}} \bar{r}_A = 0$ where $e_{B^*} \in E_\gamma$ and $\frac{\partial}{\partial \ell_{\bar{\alpha}^*}} \bar{r}_A = 0$ where $\ell_{\bar{\alpha}^*}$ is the value of a conserved charge with nonzero support in γ .

This means that reaction fluxes of all the reactions in Γ exhibit RPA with respect to the change of reaction parameters or values of conserved charges inside γ

if $\lambda_f(\gamma) = 0$. Notably, the adaptation is robust, meaning that it does not require any fine-tuning of parameters. This robustness is a consequence of the fact that the condition of vanishing index is determined only by the topology of the network and is insensitive to the details of the reactions. We refer to a subnetwork γ with $\lambda_f(\gamma) = 0$ as a *strong buffering structure*. A reaction network can contain multiple strong buffering structures. As we show in the SM, strong buffering structures are closed under union and intersection: if γ_1 and γ_2 are strong buffering structures, so are $\gamma_1 \cup \gamma_2$ and $\gamma_1 \cap \gamma_2$. We say that a strong buffering structure is *maximal* if it contains all the strong buffering structures in the network.

Example 1.—As a simple example, let us consider the following reaction network Γ with four species and six reactions,



See the left part of Fig. 1 for the visual representation of the network. The network contains seven strong buffering structures (see the SM for details). Among them, $\gamma_7^* = (\{v_1, v_2, v_4\}, \{e_2, e_3, e_5\})$ has a zero flux influence index ($\lambda_f(\gamma) = -3 + 3 + 0 = 0$) and is maximal. Theorem 1 predicts that reaction fluxes exhibit RPA with respect to parameters k_2, k_3, k_5 . Indeed, if we for example employ the mass-action kinetics and solve for the steady-state reaction fluxes, they only depend on k_1, k_4 , and k_6 :

$$\bar{\mathbf{r}} = k_1 \mathbf{c}^{(1)} + \frac{k_4 k_1}{k_6} \mathbf{c}^{(2)}, \quad (7)$$

where $\mathbf{c}^{(1)} := [1 \ 1 \ 0 \ 1 \ 0 \ 1]^\top$ and $\mathbf{c}^{(2)} := [1 \ 1 \ 1 \ 0 \ 1 \ 0]^\top$ are basis vectors of $\ker S$ (the component are arranged in the order of $\{e_2, e_3, e_5, e_1, e_4, e_6\}$ for later convenience).

Minimal form.—Combining the notion of strong buffering structures with the reduction method introduced in Ref. [18], we can define a simpler yet faithful representation of complex reaction networks, in the sense that the steady-state fluxes of the original system can be fully recovered from those of the simplified system.

Let us describe the construction of a reduced reaction system. For a chosen output-complete subnetwork γ , we separate the chemical concentrations and reaction fluxes into those inside/outside γ as

$$\mathbf{x} = \begin{pmatrix} \mathbf{x}_1 \\ \mathbf{x}_2 \end{pmatrix}, \quad \mathbf{r} = \begin{pmatrix} \mathbf{r}_1 \\ \mathbf{r}_2 \end{pmatrix}, \quad (8)$$

¹ We provide the proofs of Theorems 1 & 2 in the Supplemental Material (SM).

where 1 and 2 correspond to inside and outside degrees of freedom, respectively. Accordingly to this separation of species/reactions, the stoichiometric matrix S is partitioned into four blocks as

$$S = \begin{pmatrix} S_{11} & S_{12} \\ S_{21} & S_{22} \end{pmatrix}. \quad (9)$$

In the reduced system, the species and reactions inside γ are eliminated. The rate equation of the reduced reaction system is written as

$$\frac{d}{dt} \mathbf{x}_2 = S' \mathbf{r}_2(\mathbf{x}_2), \quad (10)$$

where S' is the so-called generalized Schur complement of S with respect to S_{11} ,

$$S' := S_{22} - S_{21} S_{11}^+ S_{12}. \quad (11)$$

Here, S_{11}^+ is the Moore-Penrose inverse of S_{11} . We will denote the reduced network obtained by removing γ from Γ as $\Gamma' := \Gamma/\gamma$. The structure of the reduced network is characterized by S' , and the second term of Eq. (11) is responsible for the reconnections of reactions associated with the removal of subnetwork γ .

For a given reaction network Γ , its *minimal form* Γ_{\min} is a reaction system obtained by reducing the maximal strong buffering structure in Γ in the sense described above. We can show the following:²

Theorem 2 (Reconstruction of steady-state reaction fluxes from the minimal form). Let Γ be a reaction system and Γ_{\min} be its minimal form. Then, the steady-state reaction fluxes of Γ can be reconstructed from those of Γ_{\min} .

We provide a proof in the SM.

Let us illustrate the reconstruction procedure. Suppose that the steady-state reaction flux in Γ_{\min} is given by

$$\bar{\mathbf{r}}_2 = \sum_{\alpha} \mu^{(\alpha)} \mathbf{c}_2^{(\alpha)}, \quad (12)$$

where $\{\mathbf{c}_2^{(\alpha)}\}_{\alpha}$ is a basis of $\ker S'$, and the coefficients $\mu^{(\alpha)} = \mu^{(\alpha)}(\mathbf{k}_2)$ are functions of the reaction parameters outside γ . When γ is a strong buffering structure, there is an isomorphism f from $\ker S'$ to $\ker S$,

$$\ker S' \ni \mathbf{c}_2 \mapsto f(\mathbf{c}_2) = \begin{bmatrix} -S_{11}^+ S_{12} \mathbf{c}_2 \\ \mathbf{c}_2 \end{bmatrix} \in \ker S. \quad (13)$$

Using this map, the steady-state reaction flux of the original system is reconstructed by

$$\bar{\mathbf{r}} = \sum_{\alpha} \mu^{(\alpha)} f(\mathbf{c}_2^{(\alpha)}), \quad (14)$$

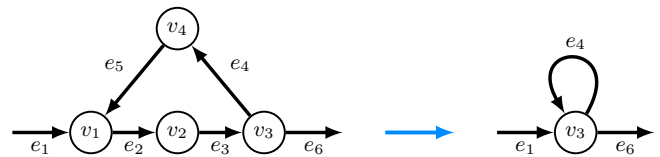


FIG. 1: Simple example of reduction to the minimal form (Example 1). The left network is the original one, and the right one is the corresponding minimal form.

where the coefficients $\mu^{(\alpha)}$ are the same as Eq. (12).

In Example 1, γ_7^* is maximal, and the minimal form is obtained as $\Gamma_{\min} = \Gamma/\gamma_7^*$. Under the reduction $\Gamma \rightarrow \Gamma_{\min}$, the stoichiometric matrix changes as

$$S = \begin{matrix} v_1 \\ v_2 \\ v_4 \\ v_3 \end{matrix} \begin{matrix} \begin{matrix} S_{11} \\ \hline \end{matrix} \\ \begin{bmatrix} -1 & 0 & 1 & 1 & 0 & 0 \\ 1 & -1 & 0 & 0 & 0 & 0 \\ 0 & 0 & -1 & 0 & 1 & 0 \\ 0 & 1 & 0 & 0 & -1 & -1 \end{bmatrix} \end{matrix} \begin{matrix} e_2 \\ e_3 \\ e_5 \\ e_1 \\ e_4 \\ e_6 \end{matrix} \longrightarrow S' = v_3 \begin{bmatrix} 1 & 0 & -1 \\ e_1 & e_4 & e_6 \end{bmatrix} \quad (15)$$

where we have brought the components in γ_7^* to the upper-left part. The reduction can be visually represented as Fig. 1.

We can easily compute the steady-state reaction fluxes of the original system using its minimal form. A set of basis vectors of $\ker S'$ can be picked as $\mathbf{c}_2^{(1)} = [1 \ 0 \ 1]^\top$, and $\mathbf{c}_2^{(2)} = [0 \ 1 \ 0]^\top$, where the elements are in the order of $\{e_1, e_4, e_6\}$. The rate equation of the reduced system involves only one species and is given by

$$\frac{d}{dt} x_3 = k_1 - k_6 x_3, \quad (16)$$

where we have chosen the mass-action kinetics. At the steady state, $\bar{x}_3 = k_1/k_6$. Since $r_4 = k_4 x_3$, its steady-state value is determined as $\bar{r}_4 = k_4 k_1/k_6$. Hence, the steady-state reaction fluxes in the reduced system are given by

$$\bar{\mathbf{r}}_2 = k_1 \mathbf{c}_2^{(1)} + \frac{k_4 k_1}{k_6} \mathbf{c}_2^{(2)}. \quad (17)$$

Using the map (13), the steady-state reaction fluxes of the original system is obtained. Indeed, $\mathbf{c}_1^{(1)}$ and $\mathbf{c}_1^{(2)}$ in Eq. (7) are the images of $\mathbf{c}_2^{(1)}$ and $\mathbf{c}_2^{(2)}$ via the map (13), i. e. $\mathbf{c}_1^{(1)} = f(\mathbf{c}_2^{(1)})$ and $\mathbf{c}_1^{(2)} = f(\mathbf{c}_2^{(2)})$.

Metabolic pathways of E. coli.—As a realistic example, here we consider the metabolic pathways [20, 24] of *E. coli*. The whole network Γ is shown in Fig. 2(a), which consists of the glycolysis, the pentose phosphate pathway, and the tricarboxylic acid cycle. This network contains 12 generators of strong buffering structures (note that the unions of them are also strong buffering structures).

² We make a technical assumption on the nature of conserved charges in the system. See the SM for details.

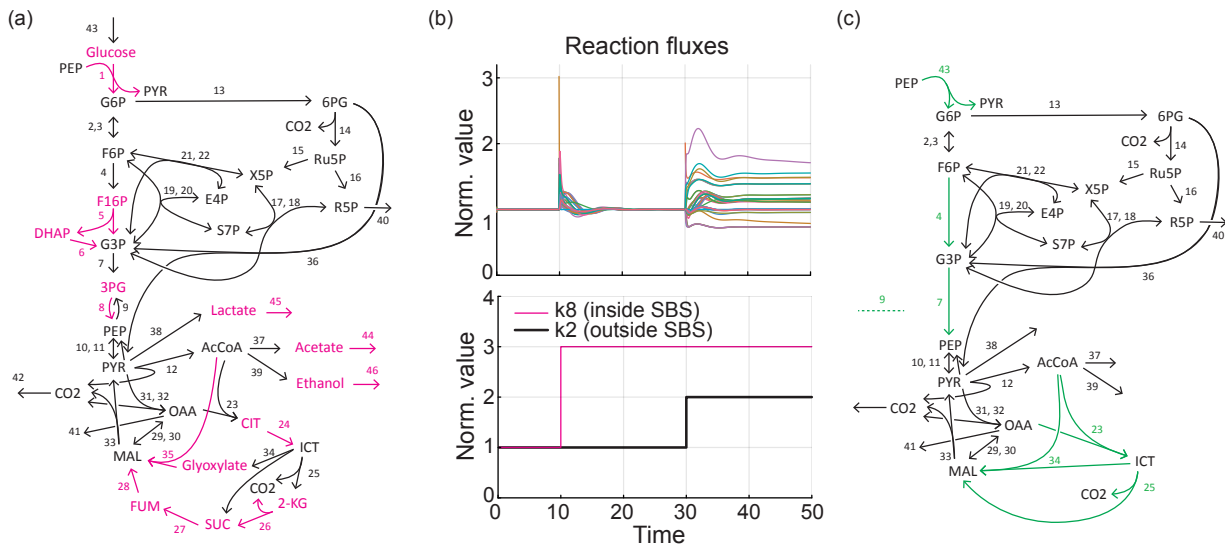


FIG. 2: (a) Central metabolic pathways of *E. coli*. The magenta-colored subnetwork is the maximal buffering structure. (b) Time-series of reaction fluxes of all 46 reactions. After perturbing parameter k_8 , inside the maximal strong buffering structure, at time $t = 10$, all reaction fluxes exhibit RPA. After perturbing parameter k_2 , outside the maximal strong buffering structure, at time $t = 30$, the reaction fluxes are changed. (c) The minimal form of the network in (a). The green-colored reactions are the reconnected ones after the reduction.

The maximal one, $\bar{\gamma}_s$, is the union of all the 12 subnetworks (Fig. 2(a); magenta-colors). All the reaction fluxes at the steady-state are insensitive to 12 parameters in $\bar{\gamma}_s$. For instance, when k_8 in $\bar{\gamma}_s$ is perturbed, all the reaction fluxes are adapted to the original steady states (Fig. 2(b)). On the other hand, such RPA does not occur when k_2 outside $\bar{\gamma}_s$ is perturbed (Fig. 2(b)). In Fig. 2(c), we present the minimal form $\Gamma_{\min} := \Gamma/\bar{\gamma}_s$. While the original system contains 28 species and 46 reactions, the reduced system has 16 species and 34 reactions. The steady-state reaction fluxes of Γ can be exactly reconstructed from the smaller system Γ_{\min} . The reduced system is simpler to analyze and is helpful for us to identify relevant parameters for determining reaction fluxes, which can be useful for flux balance analysis [22, 25–27].

Summary and discussions.—In this Letter, we have identified the structural condition under which all the reaction fluxes show RPA with respect to the parameters inside a subnetwork γ : this is achieved when γ is output-complete and has vanishing flux influence index $\lambda_f(\gamma) = 0$ introduced in Eq. (4). Identifying strong buffering structures is particularly useful for the analysis of large reaction networks, as the parameters inside these subnetworks are irrelevant in determining the steady-state reaction fluxes and can be disregarded from the start. Theorem 1 provides us with a constraint from the network topology on the response of reaction systems against parameter perturbations and would be helpful in understanding the results of, for example, metabolic control analysis [28–32]. We gave a method for obtaining the corresponding reduced system (minimal form), which is

the tightest expression of the original reaction network without losing any information about the steady-state reaction fluxes. Since the condition of vanishing index is a topological one and is insensitive to the details of reactions such as reaction kinetics and parameter values, the results hold for any kinetics/parameters and thus are broadly applicable.

Finally, let us comment on the relation of strong buffering structures to buffering structures defined by the vanishing of the influence index, $\lambda(\gamma)$ [16–18]. When a subnetwork has a vanishing influence index $\lambda(\gamma) = 0$, the concentrations and reaction fluxes outside γ exhibit RPA with respect to the parameters inside γ . Strong buffering structures are a restricted type of buffering structures, and *all* the reaction fluxes show RPA for the parameters inside γ if $\lambda_f(\gamma) = 0$. As we show in the SM, a strong one is always a usual buffering structure: $\lambda_f(\gamma) = 0$ implies $\lambda(\gamma) = 0$.

YH is supported by an appointment of the JRG Program at the APCTP, which is funded through the Science and Technology Promotion Fund and Lottery Fund of the Korean Government, and is also supported by the Korean Local Governments of Gyeongsangbuk-do Province and Pohang City. YH is also supported by the National Research Foundation (NRF) of Korea (Grant No. 2020R1F1A1076267) funded by the Korean Government (MSIT). HH is supported by the National Research Foundation of Korea (NRF) NRF-2019- Fostering Core Leaders of the Future Basic Science Program/Global Ph.D. Fellowship Program 2019H1A2A1075303. JKK is supported by the Institute for Basic Science IBS-R029-C3.

-
- * yuji.hirono@gmail.com
† hphong@kaist.ac.kr
‡ jaekkim@kaist.ac.kr
- [1] H. Kitano, Biological robustness, *Nature Reviews Genetics* **5**, 826 (2004).
- [2] H. Kitano, Towards a theory of biological robustness, *Molecular systems biology* **3**, 137 (2007).
- [3] N. Barkai and S. Leibler, Robustness in simple biochemical networks, *Nature* **387**, 913 (1997).
- [4] U. Alon, M. G. Surette, N. Barkai, and S. Leibler, Robustness in bacterial chemotaxis, *Nature* **397**, 168 (1999).
- [5] J. E. Ferrell, Perfect and near-perfect adaptation in cell signaling, *Cell Systems* **2**, 62 (2016).
- [6] S. K. Aoki, G. Lillacci, A. Gupta, A. Baumschlager, D. Schweingruber, and M. Khammash, A universal biomolecular integral feedback controller for robust perfect adaptation, *Nature* **570**, 533 (2019).
- [7] M. H. Khammash, Perfect adaptation in biology, *Cell Systems* **12**, 509 (2021).
- [8] M. Kanehisa and S. Goto, KEGG: Kyoto Encyclopedia of Genes and Genomes, *Nucleic Acids Research* **28**, 27 (2000).
- [9] H. Jeong, B. Tombor, R. Albert, Z. N. Oltvai, and A.-L. Barabási, The large-scale organization of metabolic networks, *Nature* **407**, 651 (2000).
- [10] E. Ravasz, A. L. Somera, D. A. Mongru, Z. N. Oltvai, and A.-L. Barabási, Hierarchical organization of modularity in metabolic networks, *science* **297**, 1551 (2002).
- [11] T.-M. Yi, Y. Huang, M. I. Simon, and J. Doyle, Robust perfect adaptation in bacterial chemotaxis through integral feedback control, *Proceedings of the National Academy of Sciences* **97**, 4649 (2000).
- [12] F. Xiao and J. C. Doyle, Robust perfect adaptation in biomolecular reaction networks, in *2018 IEEE Conference on Decision and Control (CDC)* (2018) pp. 4345–4352.
- [13] R. P. Araujo and L. A. Liotta, The topological requirements for robust perfect adaptation in networks of any size, *Nature communications* **9**, 1 (2018).
- [14] Y. Wang, Z. Huang, F. Antoneli, and M. Golubitsky, The structure of infinitesimal homeostasis in input–output networks, *Journal of mathematical biology* **82**, 1 (2021).
- [15] A. Gupta and M. Khammash, Universal structural requirements for maximal robust perfect adaptation in biomolecular networks, bioRxiv [10.1101/2022.02.01.478605](https://doi.org/10.1101/2022.02.01.478605) (2022).
- [16] T. Okada and A. Mochizuki, Law of localization in chemical reaction networks, *Phys. Rev. Lett.* **117**, 048101 (2016).
- [17] T. Okada and A. Mochizuki, Sensitivity and network topology in chemical reaction systems, *Phys. Rev. E* **96**, 022322 (2017).
- [18] Y. Hirono, T. Okada, H. Miyazaki, and Y. Hidaka, Structural reduction of chemical reaction networks based on topology, *Phys. Rev. Research* **3**, 043123 (2021).
- [19] A. Mochizuki and B. Fiedler, Sensitivity of chemical reaction networks: A structural approach. 1. examples and the carbon metabolic network, *Journal of Theoretical Biology* **367**, 189 (2015).
- [20] B. Fiedler and A. Mochizuki, Sensitivity of chemical reaction networks: a structural approach. 2. regular monomolecular systems, *Mathematical Methods in the Applied Sciences* **38**, 3519 (2015).
- [21] B. Brehm and B. Fiedler, Sensitivity of chemical reaction networks: A structural approach. 3. regular multimolecular systems, *Mathematical Methods in the Applied Sciences* **41**, 1344 (2018).
- [22] J. D. Orth, I. Thiele, and B. Ø. Palsson, What is flux balance analysis?, *Nature biotechnology* **28**, 245 (2010).
- [23] I. Famili and B. O. Palsson, The convex basis of the left null space of the stoichiometric matrix leads to the definition of metabolically meaningful pools, *Biophysical Journal* **85**, 16 (2003).
- [24] N. Ishii, K. Nakahigashi, T. Baba, M. Robert, T. Soga, A. Kanai, T. Hirasawa, M. Naba, K. Hirai, A. Hoque, *et al.*, Multiple high-throughput analyses monitor the response of *e. coli* to perturbations, *Science* **316**, 593 (2007).
- [25] E. P. Gianchandani, A. K. Chavali, and J. A. Papin, The application of flux balance analysis in systems biology, *WIREs Systems Biology and Medicine* **2**, 372 (2010).
- [26] K. Raman and N. Chandra, Flux balance analysis of biological systems: applications and challenges, *Briefings in Bioinformatics* **10**, 435 (2009).
- [27] K. J. Kauffman, P. Prakash, and J. S. Edwards, Advances in flux balance analysis, *Current Opinion in Biotechnology* **14**, 491 (2003).
- [28] H. Kacser and J. Burns, The control of flux., in *Symposia of the Society for Experimental Biology*, Vol. 27 (1973) p. 65.
- [29] D. A. Fell, Metabolic control analysis: a survey of its theoretical and experimental development, *Biochemical Journal* **286**, 313 (1992).
- [30] E. Szathmary, Do deleterious mutations act synergistically? metabolic control theory provides a partial answer., *Genetics* **133**, 127 (1993).
- [31] R. MacLean, Predicting epistasis: an experimental test of metabolic control theory with bacterial transcription and translation, *Journal of evolutionary biology* **23**, 488 (2010).
- [32] H. C. Bagheri and G. P. Wagner, Evolution of dominance in metabolic pathways, *Genetics* **168**, 1713 (2004).

Supplemental Material for “Robust Perfect Adaptation of Reaction Fluxes Ensured by Network Topology”

NOTATIONS

In the following, the sets of chemical species and reactions are denoted by V and E , respectively. For a given species $v_i \in V$ and reaction $e_A \in E$, the corresponding concentration and reaction rate will be denoted by x_i and r_A , respectively. The cardinality of a set V is indicated by $|V|$. The dimension of a vector space W is denoted by $|W|$. For a given set of vectors, $\mathbf{v}_1, \mathbf{v}_2, \dots$, $\text{span}\{\mathbf{v}_1, \mathbf{v}_2, \dots\}$ indicates the vector space spanned by them.

RELATION OF THE FLUX INFLUENCE INDEX AND INFLUENCE INDEX

Here, we discuss the relationship between the flux influence index $\lambda_f(\gamma)$ introduced in this work and the influence index $\lambda(\gamma)$ [1-3]. These two indices are related by

$$\lambda_f(\gamma) = \lambda(\gamma) + |(\ker S)_{\text{supp } \gamma}|, \quad (18)$$

where the last term is the dimension of the following vector space,

$$(\ker S)_{\text{supp } \gamma} := \{\mathbf{c} \mid \mathbf{c} \in \ker S, P_\gamma^1 \mathbf{c} = \mathbf{c}\}. \quad (19)$$

Here, P_γ^1 is the projection matrix to γ in the space of chemical reactions. Intuitively speaking, $(\ker S)_{\text{supp } \gamma}$ is the space of cycles that are supported inside subnetwork γ . Noting that $\lambda(\gamma)$ is nonnegative for reaction systems with asymptotically stable steady states, $\lambda_f(\gamma) = 0$ implies $\lambda(\gamma) = 0$. Thus, a strong buffering structure is always a buffering structure.

CLOSURE PROPERTY OF STRONG BUFFERING STRUCTURES

We first prove the submodularity of the flux influence index. It consequently implies that strong buffering structures are closed under the union and intersection.

Proposition 1 (Submodularity of the flux influence index). The following inequality holds for any two subnetworks γ_1 and γ_2 ,

$$\lambda_f(\gamma_1) + \lambda_f(\gamma_2) \geq \lambda_f(\gamma_1 \cap \gamma_2) + \lambda_f(\gamma_1 \cup \gamma_2). \quad (20)$$

Proof. By definition, the flux influence indices are given by

$$\lambda_f(\gamma_1 \cap \gamma_2) = -|V_{\gamma_1 \cap \gamma_2}| + |E_{\gamma_1 \cap \gamma_2}| + |P_{\gamma_1 \cap \gamma_2}^0(\text{coker } S)|, \quad (21)$$

$$\lambda_f(\gamma_1 \cup \gamma_2) = -|V_{\gamma_1 \cup \gamma_2}| + |E_{\gamma_1 \cup \gamma_2}| + |P_{\gamma_1 \cup \gamma_2}^0(\text{coker } S)|. \quad (22)$$

By summing these two, we get

$$\begin{aligned} \lambda_f(\gamma_1 \cap \gamma_2) + \lambda_f(\gamma_1 \cup \gamma_2) &= -(|V_{\gamma_1 \cap \gamma_2}| + |V_{\gamma_1 \cup \gamma_2}|) + |E_{\gamma_1 \cap \gamma_2}| + |E_{\gamma_1 \cup \gamma_2}| + |P_{\gamma_1 \cap \gamma_2}^0(\text{coker } S)| + |P_{\gamma_1 \cup \gamma_2}^0(\text{coker } S)| \\ &= -(|V_{\gamma_1}| + |V_{\gamma_2}|) + |E_{\gamma_1}| + |E_{\gamma_2}| + |P_{\gamma_1 \cap \gamma_2}^0(\text{coker } S)| + |P_{\gamma_1 \cup \gamma_2}^0(\text{coker } S)| \\ &= \lambda_f(\gamma_1) + \lambda_f(\gamma_2) - |P_{\gamma_1}^0(\text{coker } S)| - |P_{\gamma_2}^0(\text{coker } S)| + |P_{\gamma_1 \cap \gamma_2}^0(\text{coker } S)| + |P_{\gamma_1 \cup \gamma_2}^0(\text{coker } S)| \\ &\leq \lambda_f(\gamma_1) + \lambda_f(\gamma_2). \end{aligned} \quad (23)$$

The last inequality holds because $|P_\gamma^0(\text{coker } S)|$ is a submodular function, i.e., $|P_{\gamma_1}^0(\text{coker } S)| + |P_{\gamma_2}^0(\text{coker } S)| \geq |P_{\gamma_1 \cap \gamma_2}^0(\text{coker } S)| + |P_{\gamma_1 \cup \gamma_2}^0(\text{coker } S)|$, as shown in a previous work [3]. Consequently, the flux influence index is also a submodular function. \square

Corollary 2 (Closure property of strong buffering structures). If γ and γ_2 are strong buffering structures, then both $\gamma_1 \cap \gamma_2$ and $\gamma_1 \cup \gamma_2$ are strong buffering structures.

Proof. To prove that the intersection and union are strong buffering structures, we need to show that they are output-complete and their flux influence indices are zero. The output-completeness is clearly guaranteed after taking the intersection and union. Since the flux influence indices are always nonnegative, $\lambda_f(\gamma_1) = \lambda_f(\gamma_2) = 0$ implies that $\lambda_f(\gamma_1 \cap \gamma_2) = \lambda_f(\gamma_1 \cup \gamma_2) = 0$ by the submodularity of the flux influence index (Proposition 1), which means that the intersection and union are strong buffering structures. \square

PROOF OF THEOREM 1

We assume that the system reaches a steady state in the long time limit, and the chemical concentrations at the steady state are determined uniquely for a given set of rate parameters and the values of conserved charges, $\{k_A, \ell^{\bar{\alpha}}\}$. At the steady state, the reaction rates and the concentrations satisfy³

$$\sum_A S_{iA} r_A(\mathbf{x}(\mathbf{k}, \boldsymbol{\ell}), k_A) = 0, \quad (24)$$

$$\sum_i d_i^{(\bar{\alpha})} x_i(\mathbf{k}, \boldsymbol{\ell}) = \ell^{\bar{\alpha}}, \quad (25)$$

where $\{d^{(\bar{\alpha})}\}_{\bar{\alpha}=1, \dots, |\bar{\alpha}|}$ is a basis of coker S , and the second equation specifies the values of conserved charges. We assume the existence of an asymptotically stable steady state, and we study how the state changes under the change of parameters. The concentrations and reaction rates are determined by solving Eqs. (24) and (25). Note that steady-state reaction rates $r_A(\mathbf{x}(\mathbf{k}, \boldsymbol{\ell}), k_A)$ have an explicit dependence on k_A , as well as an implicit dependence on \mathbf{k} and $\boldsymbol{\ell}$ through steady-state concentrations, $x_i(\mathbf{k}, \boldsymbol{\ell})$. Equation (24) indicates that the steady-state reaction rates are in the kernel of matrix S . Hence, the rates can be written as

$$r_A(\mathbf{x}(\mathbf{k}, \boldsymbol{\ell}), k_A) = \sum_{\alpha} \mu_{\alpha}(\mathbf{k}, \boldsymbol{\ell}) c_A^{(\alpha)}. \quad (26)$$

where $\{c^{(\alpha)}\}_{\alpha=1, \dots, |\alpha|}$ is a basis of $\ker S$. Taking the derivative of Eqs. (26) and (25) with respect to k_B and $\ell^{\bar{\beta}}$, we have

$$\sum_i \frac{\partial r_A}{\partial x_i} \frac{\partial x_i}{\partial k_B} + \frac{\partial r_A}{\partial k_B} = \sum_{\alpha} \frac{\partial \mu_{\alpha}}{\partial k_B} c_A^{(\alpha)}, \quad (27)$$

$$\sum_i \frac{\partial r_A}{\partial x_i} \frac{\partial x_i}{\partial \ell^{\bar{\beta}}} = \sum_{\alpha} \frac{\partial \mu_{\alpha}}{\partial \ell^{\bar{\beta}}} c_A^{(\alpha)}, \quad (28)$$

$$\sum_i d_i^{(\bar{\alpha})} \frac{\partial x_i}{\partial k_B} = 0, \quad (29)$$

$$\sum_i d_i^{(\bar{\alpha})} \frac{\partial x_i}{\partial \ell^{\bar{\beta}}} = \delta^{\bar{\alpha}\bar{\beta}}. \quad (30)$$

Here, $\frac{\partial r_A}{\partial k_B}$ indicates the derivative with respect to the *explicit* dependence, and $\frac{\partial r_A}{\partial x_i}$ is evaluated at the steady state. We introduce a square matrix by

$$\mathbf{A} := \begin{pmatrix} \partial_i r_A & -c_A^{(\alpha)} \\ d_i^{(\bar{\alpha})} & \mathbf{0} \end{pmatrix}, \quad (31)$$

where $\partial_i := \partial/\partial x_i$. Using this, Eqs. (27–30) are summarized in a compact way in matrix form,

$$\mathbf{A} \begin{pmatrix} \partial_B x_i \\ \partial_B \mu_{\alpha} \end{pmatrix} = - \begin{pmatrix} \partial_B r_A \\ \mathbf{0} \end{pmatrix}, \quad \mathbf{A} \begin{pmatrix} \partial_{\bar{\beta}} x_i \\ \partial_{\bar{\beta}} \mu_{\alpha} \end{pmatrix} = \begin{pmatrix} \mathbf{0} \\ \delta^{\bar{\alpha}\bar{\beta}} \end{pmatrix}, \quad (32)$$

³ Here we use different characters for indices of chemical species (i, j, \dots), reactions (A, B, \dots), the basis of the kernel of S (α, β, \dots), and that of cokernel of S ($\bar{\alpha}, \bar{\beta}, \dots$). We use the notation where $|i|$ indicates the number of values the index i takes. Thus, $|i|$ indicates the number of chemical species and $|A|$ indicates the number of reactions.

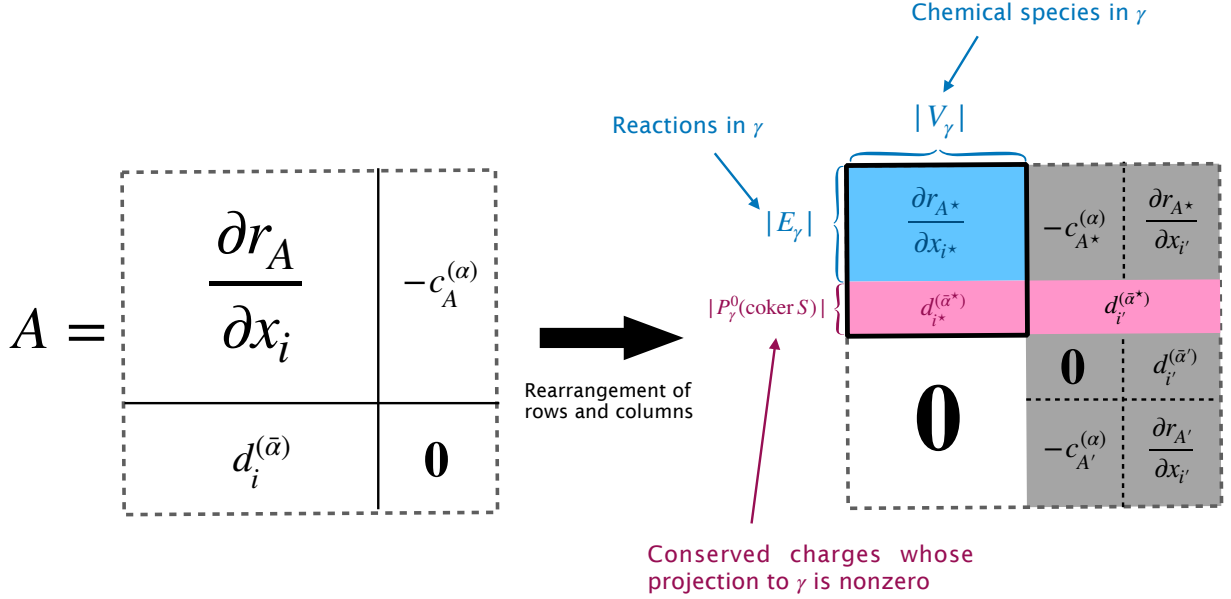


FIG. 3: Structure of the \mathbf{A} -matrix before and after a rearrangement of rows and columns. Indices with stars are those inside γ , and indices with primes are associated with $\Gamma \setminus \gamma$. The vectors $\mathbf{d}^{(\bar{\alpha}^*)}$ are the elements of $\text{coker } S$ whose projections to subnetwork γ are nonzero.

where $\partial_B := \partial/\partial k^B$, $\partial_{\bar{\beta}} := \partial/\partial \ell^{\bar{\beta}}$. By multiplying \mathbf{A}^{-1} on Eq. (32), we have

$$\partial_B \begin{pmatrix} x_i \\ \mu_\alpha \end{pmatrix} = -\mathbf{A}^{-1} \begin{pmatrix} \partial_{B^r A} \\ \mathbf{0} \end{pmatrix}, \quad \partial_{\bar{\beta}} \begin{pmatrix} x_i \\ \mu_\alpha \end{pmatrix} = \mathbf{A}^{-1} \begin{pmatrix} \mathbf{0} \\ \delta_{\bar{\alpha}\bar{\beta}} \end{pmatrix}. \quad (33)$$

Note that $\partial_{B^r A}$ is a diagonal matrix, i.e., $\partial_{B^r A} \propto \delta_{BA}$. If we partition \mathbf{A}^{-1} as

$$\mathbf{A}^{-1} = \begin{pmatrix} (\mathbf{A}^{-1})_{iA} & (\mathbf{A}^{-1})_{i\bar{\alpha}} \\ (\mathbf{A}^{-1})_{\alpha A} & (\mathbf{A}^{-1})_{\alpha\bar{\alpha}} \end{pmatrix}, \quad (34)$$

the responses of steady-state concentrations and reaction rates to the perturbations of k_B and $\ell^{\bar{\beta}}$ are proportional to the following components,

$$\partial_B x_i \propto (\mathbf{A}^{-1})_{iB}, \quad \partial_{\bar{\beta}} x_i \propto (\mathbf{A}^{-1})_{i\bar{\beta}}, \quad \partial_B \mu_\alpha \propto (\mathbf{A}^{-1})_{\alpha B}, \quad \partial_{\bar{\beta}} \mu_\alpha \propto (\mathbf{A}^{-1})_{\alpha\bar{\beta}}. \quad (35)$$

For a given output-complete subnetwork γ , we can bring the rows and columns associated with γ to the upper-left corner (see Fig. 3). All the component of the lower-left part is zero, because the reaction rate r_A outside γ does not depend on the chemical species in γ (since γ is output-complete). When $\lambda_f(\gamma) = 0$, the black box in the upper-left corner is a square matrix. Then, \mathbf{A}^{-1} inherits the same structure,

$$\mathbf{A}^{-1} = \begin{pmatrix} * & * \\ \mathbf{0} & * \end{pmatrix}. \quad (36)$$

Namely, if we denote the generic index of \mathbf{A}^{-1} as μ, ν, \dots and write the index inside and outside γ as μ^* and μ' , respectively, we have $(\mathbf{A}^{-1})_{\mu'\nu^*} = 0$. Because of this structure,

$$\partial_{A^*} \mu_\alpha \propto (\mathbf{A}^{-1})_{\alpha A^*} = 0, \quad \partial_{\bar{\alpha}^*} \mu_\alpha \propto (\mathbf{A}^{-1})_{\alpha \bar{\alpha}^*} = 0, \quad (37)$$

for *any* α . Thus, all the steady-state reaction rates are independent of the parameters inside strong buffering structures and the values of conserved charges that have nonzero support inside γ .

PROOF OF THEOREM 2

We make the following technical assumptions on the nature of conserved charges:

Assumption 3. For a given element \mathbf{d} of $\text{coker } S$, let us separate \mathbf{d} into those inside/outside the maximal strong buffering structure γ as $\mathbf{d} = \begin{bmatrix} \mathbf{d}_1 \\ \mathbf{d}_2 \end{bmatrix}$. Then, if $\mathbf{d}_1 \in \text{coker } S_{11}$, $\begin{bmatrix} \mathbf{d}_1 \\ \mathbf{0} \end{bmatrix} \in \text{coker } S$ holds.

Namely, a local conserved charge in a subnetwork γ (i.e. an element of $\text{coker } S_{11}$) is always a conserved charge in the whole network Γ . We here give a proof that Theorem 2 holds under Assumption 3. In Sec. , we introduce a long exact sequence which will be used in the proof. We will complete the proof in Sec. .

Long exact sequence of a pair of chemical reaction networks

To prove Theorem 2, we construct a reduced system using the method developed in Ref. [3] and show that the steady-state fluxes of the original system can be obtained from the reduced one. To capture the changes of cycles and conserved charges associated with a reduction, we use a long exact sequence introduced in Ref. [3].

Let us introduce its definition. We first define the spaces of chains by

$$C_0(\Gamma) := \left\{ \sum_i d_i v_i \mid v_i \in V, d_i \in \mathbb{R} \right\}, \quad (38)$$

$$C_1(\Gamma) := \left\{ \sum_A c_A e_A \mid e_A \in E, c_A \in \mathbb{R} \right\}. \quad (39)$$

Similarly, we define the spaces of chains for a subnetwork $\gamma = (V_\gamma, E_\gamma) \subset \Gamma$, $C_n(\gamma)$ for $n = 0, 1$, to be those generated by V_γ and E_γ . We also define the chain spaces of $\Gamma' = \Gamma/\gamma$, to be the spaces spanned by $(V \setminus V_\gamma, E \setminus E_\gamma)$. We will denote the elements of $C_1(\gamma)$, $C_1(\Gamma)$ and $C_1(\Gamma')$ using a vector, where each component represents the corresponding coefficient. For example,

$$\mathbf{c}_1 \in C_1(\gamma), \quad \begin{bmatrix} \mathbf{c}_1 \\ \mathbf{c}_2 \end{bmatrix} \in C_1(\Gamma), \quad \mathbf{c}_2 \in C_1(\Gamma'), \quad (40)$$

In the above, the element of $C_1(\Gamma)$ are partitioned into those inside/outside γ . A similar notation will be used for $C_0(\gamma)$ and so on. We consider the following short exact sequence of chain complexes,

$$\begin{array}{ccccccc} & & 0 & & 0 & & 0 & & & (41) \\ & & \downarrow & & \downarrow & & \downarrow & & & \\ 0 & \longrightarrow & C_1(\gamma) & \xrightarrow{\psi_1} & C_1(\Gamma) & \xrightarrow{\varphi_1} & C_1(\Gamma') & \longrightarrow & 0 \\ & & \downarrow \partial_\gamma & & \downarrow \partial & & \downarrow \partial' & & \\ 0 & \longrightarrow & C_0(\gamma) & \xrightarrow{\psi_0} & C_0(\Gamma) & \xrightarrow{\varphi_0} & C_0(\Gamma') & \longrightarrow & 0 \\ & & \downarrow & & \downarrow & & \downarrow & & \\ & & 0 & & 0 & & 0 & & \end{array}$$

where the columns are the chain complexes of γ , Γ , and Γ' , respectively. The boundary maps are given by the stoichiometric matrices of subnetwork γ , the whole network, and the reduced network⁴, respectively, as

$$\partial_\gamma : \mathbf{c}_1 \mapsto S_{11} \mathbf{c}_1, \quad \partial : \mathbf{c} = \begin{bmatrix} \mathbf{c}_1 \\ \mathbf{c}_2 \end{bmatrix} \mapsto S \mathbf{c}, \quad \partial' : \mathbf{c}_2 \mapsto S' \mathbf{c}_2. \quad (42)$$

The horizontal maps are given by

$$\psi_1 : \mathbf{c}_1 \mapsto \begin{bmatrix} \mathbf{c}_1 \\ \mathbf{0} \end{bmatrix}, \quad \varphi_1 : \begin{bmatrix} \mathbf{c}_1 \\ \mathbf{c}_2 \end{bmatrix} \mapsto \mathbf{c}_2, \quad (43)$$

⁴ Recall that the stoichiometric matrix of the reduced system is given by the generalized Schur complement, $S' := S_{22} - S_{21} S_{11}^+ S_{12}$, as discussed in the main text

$$\psi_0 : \mathbf{d}_1 \mapsto \begin{bmatrix} \mathbf{d}_1 \\ S_{21}S_{11}^+\mathbf{d}_1 \end{bmatrix}, \quad \varphi_0 : \begin{bmatrix} \mathbf{d}_1 \\ \mathbf{d}_2 \end{bmatrix} \mapsto \mathbf{d}_2 - S_{21}S_{11}^+\mathbf{d}_1. \quad (44)$$

One can check that the diagram (41) commutes when the following condition is satisfied:⁵

$$S_{21}(1 - S_{11}^+S_{11})\mathbf{c}_1 = \mathbf{0}, \quad (45)$$

where $\mathbf{c}_1 \in C_1(\gamma)$. The matrix $(1 - S_{11}^+S_{11})$ is the projection matrix to $\ker S_{11}$, and Eq. (45) is equivalent to

$$\ker S_{11} \subset \ker S_{21}. \quad (46)$$

As shown around Eq. (182) of Ref. [3], this condition is equivalent to $\tilde{c}(\gamma) = |\ker S_{11}/(\ker S)_{\text{supp } \gamma}| = 0$. Note that $\ker S_{11}$ and $(\ker S)_{\text{supp } \gamma}$ are the set of cycles in γ and cycles in Γ with components belongs to γ (see Eq. (19) for details), respectively. Thus, the number $\tilde{c}(\gamma)$ counts emergent cycles, which are cycles in γ that cannot be extended to cycles in Γ (see Ref. [3] for more details.) Thus, the diagram (41) commutes if and only if γ has no emergent cycles.

Assuming Eq. (46) holds, we can apply the snake lemma to the diagram (41) and obtain a long exact sequence⁶,

$$0 \longrightarrow \ker S_{11} \xrightarrow{\psi_1} \ker S \xrightarrow{\varphi_1} \ker S' \xrightarrow{\delta_1} \text{coker } S_{11} \xrightarrow{\bar{\psi}_0} \text{coker } S \xrightarrow{\bar{\varphi}_0} \text{coker } S' \longrightarrow 0, \quad (47)$$

where $\bar{\psi}_0$ and $\bar{\varphi}_0$ are induced maps⁷ of ψ_0 and φ_0 . The map $\delta_1 : \ker S' \rightarrow \text{coker } S_{11}$ is called the connecting map. For a given $\mathbf{c}_2 \in \ker S'$, the connecting map is given by⁸

$$\delta_1 : \mathbf{c}_2 \mapsto [S_{12}\mathbf{c}_2] \in \text{coker } S_{11}, \quad (48)$$

where [...] means to identify the differences in $\text{im } S_{11}$.

Proof of Theorem 2

Let us now describe a proof of Theorem 2.

Firstly, let us rewrite the flux influence index in a form useful for the following proof. In Ref. [3], it was shown that the influence index is decomposed as

$$\lambda(\gamma) = \tilde{c}(\gamma) + d_l(\gamma) - \tilde{d}(\gamma), \quad (49)$$

where $d_l(\gamma) := |(\text{coker } S)/X(\gamma)|$ with

$$X(\gamma) := \left\{ \begin{pmatrix} \mathbf{d}_1 \\ \mathbf{d}_2 \end{pmatrix} \in \text{coker } S \mid \mathbf{d}_1 \in \text{coker } S_{11} \right\}, \quad (50)$$

and $\tilde{d}(\gamma) := |(\text{coker } S_{11})/D_{11}(\gamma)|$ with

$$D_{11}(\gamma) := \left\{ \mathbf{d}_1 \in \text{coker } S_{11} \mid \exists \mathbf{d}_2 \text{ such that } \begin{bmatrix} \mathbf{d}_1 \\ \mathbf{d}_2 \end{bmatrix} \in \text{coker } S \right\}. \quad (51)$$

Using the relation (18) and noting that $\tilde{c}(\gamma) = |\ker S_{11}/(\ker S)_{\text{supp } \gamma}|$, we find that the flux influence index is written in the form

$$\lambda_F(\gamma) = |\ker S_{11}| + d_l(\gamma) - \tilde{d}(\gamma). \quad (52)$$

The number $\tilde{d}(\gamma)$ counts emergent conserved charges in γ , which are conserved only within γ and not in Γ . Due to Assumption 3, we have $\tilde{d}(\gamma) = 0$ and there is no emergent conserved charge in the current setting. Since $|\ker S_{11}|$ and $d_l(\gamma)$ are nonnegative, we have $|\ker S_{11}| = d_l(\gamma) = 0$. Then, $\tilde{c}(\gamma) = |\ker S_{11}/(\ker S)_{\text{supp } \gamma}| = 0$ and the diagram (41) commutes, and the long exact sequence (47) holds. Since $\tilde{d}(\gamma) = 0$, the connecting map δ_1 is a zero map⁹, and

⁵ Note that we use a notation where a unit matrix is denoted by 1.

⁶ Note that boundary operators are given by multiplications of stoichiometric matrices, so we have $\ker \partial_\gamma = \ker S_{11}$, $\ker \partial = \ker S$, and so on.

⁷ For example, $\bar{\psi}_0$ is defined as, $\text{coker } S_{11} \ni [\mathbf{d}_1] \mapsto \bar{\psi}_0([\mathbf{d}_1]) := [\psi_0(\mathbf{d}_1)] \in \text{coker } S$, where [...] indicates identifying the differences in $\text{im } S_{11}(\text{im } S)$ for $\text{coker } S_{11}(\text{coker } S)$, respectively. This map is well-defined in the sense that it does not depend on the choice of a representative $\mathbf{d}_1 \in C_0(\gamma)$, since if we had picked $\mathbf{d}_1 + S_{11}\mathbf{c}_1$, its image by ψ_0 is $\psi_0(\mathbf{d}_1 + S_{11}\mathbf{c}_1) = \psi_0(\mathbf{d}_1) + S \begin{bmatrix} \mathbf{c}_1 \\ \mathbf{0} \end{bmatrix}$ and the second term is zero in $\text{coker } S$.

⁸ The map is identified as follows. Pick an element $\mathbf{c}_2 \in \ker S'$, which can be included in $C_1(\Gamma')$. Since φ_1 is surjective, there exists $\mathbf{c} = \begin{bmatrix} \mathbf{c}_1 \\ \mathbf{c}_2 \end{bmatrix}$ such that $\varphi_1(\mathbf{c}) = \mathbf{c}_2$. From the commutativity of the diagram (41), we have $\varphi_0(S\mathbf{c}) = S'\mathbf{c}_2 = \mathbf{0}$. Since the rows of the diagram (41) are exact, there exists $\mathbf{d}_1 \in C_0(\gamma)$ such that $\psi_0(\mathbf{d}_1) = S\mathbf{c} \in \ker \varphi_0$. We obtain $[\mathbf{d}_1] = [S_{11}\mathbf{c}_1 + S_{12}\mathbf{c}_2] = [S_{12}\mathbf{c}_2] \in \text{coker } S_{11}$ by identifying the differences in $\text{im } S_{11}$. The mapping $\mathbf{c}_2 \mapsto [S_{12}\mathbf{c}_2]$ is the connecting map.

noting that $\ker S_{11} = \mathbf{0}$, we have the following exact sequence,

$$0 \longrightarrow \ker S \longrightarrow \ker S' \longrightarrow 0, \quad (53)$$

which implies the isomorphism,

$$\ker S \simeq \ker S'. \quad (54)$$

Let us explicitly construct the bijection. Suppose that we picked an element of $\ker S$,

$$\mathbf{c} = \begin{bmatrix} \mathbf{c}_1 \\ \mathbf{c}_2 \end{bmatrix} \in \ker S. \quad (55)$$

Since $\mathbf{c} \in \ker S$,

$$S\mathbf{c} = \begin{bmatrix} S_{11}\mathbf{c}_1 + S_{12}\mathbf{c}_2 \\ S_{21}\mathbf{c}_1 + S_{22}\mathbf{c}_2 \end{bmatrix} = \mathbf{0}. \quad (56)$$

We can solve this for \mathbf{c}_1 as (note that $\ker S_{11}$ is trivial) $\mathbf{c}_1 = -S_{11}^+ S_{12} \mathbf{c}_2$. Plugging this into the second equation of Eq. (56), we have

$$S' \mathbf{c}_2 = \mathbf{0}, \quad (57)$$

where $S' = S_{22} - S_{21} S_{11}^+ S_{12}$. Namely, we can get an element of $\ker S'$ from $\mathbf{c} \in \ker S$ as

$$\ker S \ni \mathbf{c} = \begin{bmatrix} \mathbf{c}_1 \\ \mathbf{c}_2 \end{bmatrix} \mapsto \mathbf{c}_2 \in \ker S'. \quad (58)$$

Conversely, for a given $\mathbf{c}_2 \in \ker S'$, we can get an element of $\ker S$ by

$$\ker S' \ni \mathbf{c}_2 \mapsto \mathbf{c} := \begin{bmatrix} -S_{11}^+ S_{12} \mathbf{c}_2 \\ \mathbf{c}_2 \end{bmatrix} \in \ker S. \quad (59)$$

Indeed,

$$S\mathbf{c} = \begin{bmatrix} (1 - S_{11} S_{11}^+) S_{12} \mathbf{c}_2 \\ S' \mathbf{c}_2 \end{bmatrix}. \quad (60)$$

The second line is zero by the assumption that $\mathbf{c}_2 \in \ker S'$. The first line of Eq. (60) also vanishes, which can be shown as follows. By Assumption 3, for a given $\mathbf{d}_1 \in \text{coker } S_{11}$, $\mathbf{d} = \begin{bmatrix} \mathbf{d}_1 \\ \mathbf{0} \end{bmatrix} \in \text{coker } S$. The condition $\mathbf{d}^\top S = \mathbf{0}$ can be expressed as follows:

$$\mathbf{d}_1^\top S_{11} = \mathbf{0}, \quad (61)$$

$$\mathbf{d}_1^\top S_{12} = \mathbf{0}. \quad (62)$$

Therefore, $\mathbf{d}_1^\top S_{12} \mathbf{c}_2 = 0$ for any $\mathbf{d}_1 \in \text{coker } S_{11}$ and $\mathbf{c}_2 \in \ker S'$. This is equivalent to $S_{12} \mathbf{c}_2 \in (\text{coker } S_{11})^\perp$. Since $(1 - S_{11} S_{11}^+)$ is a projection matrix to $\text{coker } S_{11}$, the first line of Eq. (60) vanishes. Thus, we have $S\mathbf{c} = \mathbf{0}$ and $\mathbf{c} \in \ker S$.

Thanks to the isomorphism (59), the reaction system obtained by reducing strong buffering structures can give the steady-state fluxes of the original system. Suppose that we have steady-state fluxes of Γ' ,

$$S' \mathbf{r}_2 = \mathbf{0}. \quad (63)$$

Let us pick a basis of $\ker S'$,

$$\ker S' = \text{span} \{ \mathbf{c}_2^{(\alpha)} \}_{\alpha=1 \dots |\alpha|}. \quad (64)$$

⁹ This is shown around Eq. (192) of Ref. [3].

The solution of Eq. (63) can be expanded as

$$\mathbf{r}_2 = \sum_{\alpha} \mu^{(\alpha)}(\mathbf{k}_2) \mathbf{c}_2^{(\alpha)}. \quad (65)$$

From the solution \mathbf{r}_2 , we can construct the steady-state fluxes of the whole network,

$$\mathbf{r} = \sum_{\alpha} \mu^{(\alpha)}(\mathbf{k}_2) \mathbf{c}^{(\alpha)}, \quad (66)$$

where $\mathbf{c}^{(\alpha)}$ is defined by

$$\mathbf{c}^{(\alpha)} := \begin{bmatrix} -S_{11}^+ S_{12} \mathbf{c}_2^{(\alpha)} \\ \mathbf{c}_2^{(\alpha)} \end{bmatrix}. \quad (67)$$

The steady-state fluxes constructed this way do not depend on the parameters within the strong buffering structures, \mathbf{k}_1 , because they do not appear in the rate equation of Γ' .

Although the reconstructed fluxes satisfy the steady-state condition $S\mathbf{r} = \mathbf{0}$, we should also check that the equations specifying the values of conserved charges do not give rise to additional constraints, which could invalidate the solution. The conserved charges are specified in the system Γ by

$$\mathbf{d}^{(\bar{\alpha})} \cdot \mathbf{x} = \ell^{\bar{\alpha}}. \quad (68)$$

As shown in Ref. [3], coker S can be decomposed as

$$\text{coker } S \cong (\text{coker } S)/X(\gamma) \oplus X(\gamma)/\bar{D}'(\gamma) \oplus \bar{D}'(\gamma), \quad (69)$$

where

$$\bar{D}'(\gamma) := \left\{ \begin{pmatrix} \mathbf{d}_1 \\ \mathbf{d}_2 \end{pmatrix} \in \text{coker } S \mid \mathbf{d}_1 = \mathbf{0} \right\}. \quad (70)$$

Intuitively speaking, an element of $(\text{coker } S)/X(\gamma)$ is a conserved charge in Γ whose projection to γ is not conserved in γ , an element of $X(\gamma)/\bar{D}'(\gamma)$ is a conserved charge of Γ whose projection to γ is also conserved in γ , and an element of $\bar{D}'(\gamma)$ is a conserved charge of Γ supported in $\Gamma \setminus \gamma$. Recall that $d_i(\gamma)$ is written as $d_i(\gamma) = |(\text{coker } S)/X(\gamma)|$. When $d_i(\gamma) = 0$, coker S is written as

$$\text{coker } S \cong D(\gamma) \oplus \bar{D}'(\gamma), \quad (71)$$

where we defined $D(\gamma) := X(\gamma)/\bar{D}'(\gamma)$. Correspondingly, we can divide the basis vectors of coker S into two classes, $\{\mathbf{d}^{(\bar{\alpha})}\} = \{\mathbf{d}^{(\bar{\alpha}\gamma)}, \mathbf{d}^{(\bar{\alpha}')} \}$, where $\{\mathbf{d}^{(\bar{\alpha}\gamma)}\}$ is a basis of $D(\gamma)$, and $\{\mathbf{d}^{(\bar{\alpha}')} \}$ is a basis of $\bar{D}'(\gamma)$. By Assumption 3, the basis vectors are written in the form

$$\mathbf{d}^{(\bar{\alpha}\gamma)} = \begin{pmatrix} \mathbf{d}_1^{(\bar{\alpha}\gamma)} \\ \mathbf{0} \end{pmatrix}, \quad \mathbf{d}^{(\bar{\alpha}')} = \begin{pmatrix} \mathbf{0} \\ \mathbf{d}_2^{(\bar{\alpha}')} \end{pmatrix}. \quad (72)$$

With this basis of coker S , Eq. (68) is written as

$$\mathbf{d}_1^{(\bar{\alpha}\gamma)} \cdot \mathbf{x}_1 = \ell^{\bar{\alpha}\gamma}, \quad (73)$$

$$\mathbf{d}_2^{(\bar{\alpha}')} \cdot \mathbf{x}_2 = \ell^{\bar{\alpha}'}. \quad (74)$$

In fact, $\mathbf{d}_2^{(\bar{\alpha}')}$ is a conserved charge in Γ' , $\mathbf{d}_2^{(\bar{\alpha}')} \in \text{coker } S'$, as we see below. Since $\mathbf{d}^{(\bar{\alpha}')} \in \text{coker } S$, it satisfies

$$\begin{pmatrix} \mathbf{0} & (\mathbf{d}_2^{(\bar{\alpha}')})^\top \end{pmatrix} \begin{pmatrix} S_{11} & S_{12} \\ S_{21} & S_{22} \end{pmatrix} = \begin{pmatrix} (\mathbf{d}_2^{(\bar{\alpha}')})^\top S_{21} & (\mathbf{d}_2^{(\bar{\alpha}')})^\top S_{22} \end{pmatrix} = \mathbf{0}. \quad (75)$$

This implies that $\mathbf{d}_2^{(\bar{\alpha}')}$ satisfies

$$(\mathbf{d}_2^{(\bar{\alpha}')})^\top S' = (\mathbf{d}_2^{(\bar{\alpha}')})^\top (S_{22} - S_{21} S_{11}^+ S_{12}) = \mathbf{0}, \quad (76)$$

hence $\mathbf{d}_2^{(\bar{\alpha}')} \in \text{coker } S'$. Thus we have obtained an injective map,

$$\text{coker } S \ni \mathbf{d}^{(\bar{\alpha}')} = \begin{pmatrix} \mathbf{0} \\ \mathbf{d}_2^{(\bar{\alpha}')} \end{pmatrix} \mapsto \mathbf{d}_2^{(\bar{\alpha}')} \in \text{coker } S'. \quad (77)$$

This map is nothing but the induced map $\bar{\varphi}_0$ ¹⁰, and when $\tilde{c}(\gamma) = 0$, this map is a surjection, which follows from the long exact sequence (47). The equations satisfied by the boundary part (denoted by 2) of the concentrations/rates of Γ are Eqs. (63) and (74). Since all the conserved charges in Γ' are given as images of $\bar{\varphi}_0$, the equation specifying the conserved charges is given by Eq. (74). Thus, the equations for conserved charges in Γ , Eqs. (73) and (74) do not give any additional constraints on \mathbf{x}_2 . Therefore, the steady-state rates of Γ can be obtained from those of Γ' via the map (59). This concludes the proof of Theorem 2.

DETAILS OF EXAMPLES

In this section, we give the details of the simple example discussed in the main text. We also provide a few additional illustrative examples.

Example 1

Here we consider a reaction system Γ with four species and six reactions,



The network Γ has the following nontrivial buffering structures,

$$\gamma_1^* = (\{v_1\}, \{e_2\}), \quad (81)$$

$$\gamma_2^* = (\{v_2\}, \{e_3\}), \quad (82)$$

$$\gamma_3^* = (\{v_4\}, \{e_5\}), \quad (83)$$

$$\gamma_4^* = (\{v_1, v_2\}, \{e_2, e_3\}) = \gamma_1^* \cup \gamma_2^*, \quad (84)$$

$$\gamma_5^* = (\{v_1, v_4\}, \{e_2, e_5\}) = \gamma_1^* \cup \gamma_3^*, \quad (85)$$

$$\gamma_6^* = (\{v_2, v_4\}, \{e_3, e_5\}) = \gamma_2^* \cup \gamma_3^*, \quad (86)$$

$$\gamma_7^* = (\{v_1, v_2, v_4\}, \{e_2, e_3, e_5\}) = \gamma_1^* \cup \gamma_2^* \cup \gamma_3^*, \quad (87)$$

$$\gamma_8 = (\{v_1, v_2, v_3, v_4\}, \{e_2, e_3, e_4, e_5, e_6\}). \quad (88)$$

where the ones with * are strong buffering structures, and those without * are ordinary buffering structures. Among the strong buffering structures, γ_7^* is maximal, and the minimal form is obtained as $\Gamma_{\min} = \Gamma/\gamma_7^*$. Under the reduction,

¹⁰ The map $\bar{\varphi}_0$ is written as

$$\bar{\varphi}_0 : \text{coker } S \ni \begin{bmatrix} \mathbf{d}_1 \\ \mathbf{d}_2 \end{bmatrix} \mapsto [\mathbf{d}_2 - S_{21}S_{11}^+S_{12}\mathbf{d}_2] \in \text{coker } S', \quad (78)$$

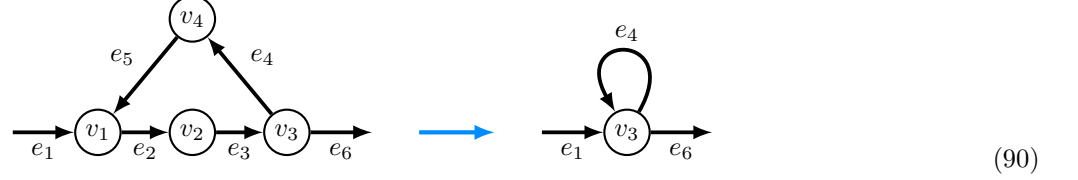
where [...] (the second one) means identifying the difference in $\text{im } S'$ or equivalently projecting to $\text{coker } S'$. The space $D(\gamma)$ is isomorphic to the kernel of $\bar{\varphi}_0$, and the nontrivial image of $\bar{\varphi}_0$ comes from $\bar{D}'(\gamma)$ in the current situation where $d_i(\gamma) = 0$. For an element $\begin{bmatrix} \mathbf{0} \\ \mathbf{d}_2 \end{bmatrix} \in \bar{D}'(\gamma)$, \mathbf{d}_2 is already in $\text{coker } S'$ as shown above, so the mapping is written as

$$\bar{\varphi}_0 : \text{coker } S \supset \bar{D}'(\gamma) \ni \begin{bmatrix} \mathbf{0} \\ \mathbf{d}_2 \end{bmatrix} \mapsto \mathbf{d}_2 \in \text{coker } S'. \quad (79)$$

the stoichiometric matrix changes as

$$S = \begin{array}{c} v_1 \\ v_2 \\ v_4 \\ v_3 \end{array} \begin{array}{c} S_{11} \\ \left[\begin{array}{ccc|ccc} -1 & 0 & 1 & 1 & 0 & 0 \\ 1 & -1 & 0 & 0 & 0 & 0 \\ 0 & 0 & -1 & 0 & 1 & 0 \\ 0 & 1 & 0 & 0 & -1 & -1 \end{array} \right] \end{array} \begin{array}{c} e_2 \ e_3 \ e_5 \\ e_1 \ e_4 \ e_6 \end{array} \longrightarrow S' = v_3 \begin{array}{c} [1 \ 0 \ -1] \\ e_1 \ e_4 \ e_6 \end{array} \quad (89)$$

where we have brought the components in γ_7^* to the upper-left part. The reduction can be visualized as



A set of basis vectors of $\ker S'$ can be picked as

$$\mathbf{c}_2^{(1)} = \begin{bmatrix} 1 \\ 0 \\ 1 \end{bmatrix}, \quad \mathbf{c}_2^{(2)} = \begin{bmatrix} 0 \\ 1 \\ 0 \end{bmatrix}, \quad (91)$$

We can use the rate equation of the reduced system to compute the steady-state rates of the original system. If we take the mass-action kinetics for example, the rate equation is

$$\frac{d}{dt}x_3 = k_1 - k_6x_3. \quad (92)$$

At the steady state, $\bar{x}_3 = k_1/k_6$, leading to $\bar{r}_6 = k_6\bar{x}_3 = k_1$ and $\bar{r}_4 = k_4\bar{x}_3 = k_4k_1/k_6$. Thus, the steady-state fluxes in the reduced system ($\bar{\mathbf{r}}_2 = [\bar{r}_1 \ \bar{r}_4 \ \bar{r}_6]^\top$) can be written as

$$\bar{\mathbf{r}}_2 = k_1\mathbf{c}_2^{(1)} + \frac{k_4k_1}{k_6}\mathbf{c}_2^{(2)}. \quad (93)$$

We can reconstruct $\mathbf{c}^{(\alpha)}$ from $\mathbf{c}_2^{(\alpha)}$; the internal components are

$$\mathbf{c}_1^{(1)} = -S_{11}^+ S_{12} \mathbf{c}_2^{(1)} = - \begin{bmatrix} -1 & 0 & -1 \\ -1 & -1 & -1 \\ 0 & 0 & -1 \end{bmatrix} \begin{bmatrix} 1 & 0 & 0 \\ 0 & 0 & 0 \\ 0 & 1 & 0 \end{bmatrix} \begin{bmatrix} 1 \\ 0 \\ 1 \end{bmatrix} = \begin{bmatrix} 1 \\ 1 \\ 0 \end{bmatrix}, \quad (94)$$

$$\mathbf{c}_1^{(2)} = -S_{11}^+ S_{12} \mathbf{c}_2^{(2)} = - \begin{bmatrix} -1 & 0 & -1 \\ -1 & -1 & -1 \\ 0 & 0 & -1 \end{bmatrix} \begin{bmatrix} 1 & 0 & 0 \\ 0 & 0 & 0 \\ 0 & 1 & 0 \end{bmatrix} \begin{bmatrix} 0 \\ 1 \\ 0 \end{bmatrix} = \begin{bmatrix} 1 \\ 1 \\ 1 \end{bmatrix}, \quad (95)$$

where the components are organized in the order $\{e_2, e_3, e_5\}$. The steady-state fluxes of the original system read

$$\bar{\mathbf{r}} = k_1\mathbf{c}^{(1)} + \frac{k_4k_1}{k_6}\mathbf{c}^{(2)}, \quad (96)$$

where

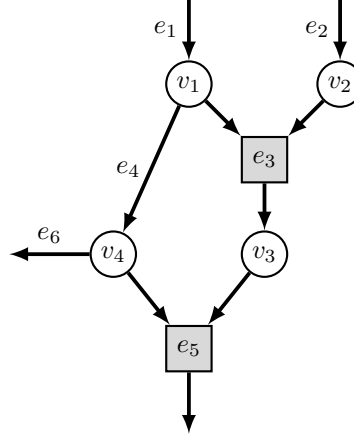
$$\mathbf{c}^{(1)} := \begin{bmatrix} \mathbf{c}_1^{(1)} \\ \mathbf{c}_2^{(1)} \end{bmatrix}, \quad \mathbf{c}^{(2)} := \begin{bmatrix} \mathbf{c}_1^{(2)} \\ \mathbf{c}_2^{(2)} \end{bmatrix}. \quad (97)$$

Example 2

We here consider the following reaction network with four species and six reactions:



The network structure is drawn as:



(99)

The stoichiometric matrix is

$$S = \begin{bmatrix} 1 & 0 & -1 & -1 & 0 & 0 \\ 0 & 1 & -1 & 0 & 0 & 0 \\ 0 & 0 & 1 & 0 & -1 & 0 \\ 0 & 0 & 0 & 1 & -1 & -1 \end{bmatrix},
 \tag{100}$$

and reaction rate functions are

$$\begin{aligned}
 \mathbf{r}(\mathbf{x}) &= [r_1 \quad r_2 \quad r_3(x_1, x_2) \quad r_4(x_1) \quad r_5(x_3, x_4) \quad r_6(x_4)]^\top \\
 &= [k_1 \quad k_2 \quad k_3 x_1 x_2 \quad k_4 x_1 \quad k_5 x_3 x_4 \quad k_6 x_4]^\top.
 \end{aligned}
 \tag{101}$$

We can identify all the nontrivial buffering structures in this example as

$$\gamma_1^* = (\{v_2\}, \{e_3\}),
 \tag{102}$$

$$\gamma_2^* = (\{v_3\}, \{e_5\}),
 \tag{103}$$

$$\gamma_3^* = (\{v_1, v_2\}, \{e_3, e_4\}),
 \tag{104}$$

$$\gamma_4^* = (\{v_2, v_3\}, \{e_3, e_5\}) = \gamma_1^* \cup \gamma_2^*,
 \tag{105}$$

$$\gamma_5^* = (\{v_3, v_4\}, \{e_5, e_6\}),
 \tag{106}$$

$$\gamma_6^* = (\{v_1, v_2, v_3\}, \{e_3, e_4, e_5\}) = \gamma_2^* \cup \gamma_3^*,
 \tag{107}$$

$$\gamma_7^* = (\{v_2, v_3, v_4\}, \{e_3, e_5, e_6\}),
 \tag{108}$$

$$\gamma_8^* = (\{v_1, v_2, v_3, v_4\}, \{e_3, e_4, e_5, e_6\}) = \gamma_3^* \cup \gamma_5^*.
 \tag{109}$$

All the eight buffering structures are strong buffering structures. Among these, γ_8^* is maximal, i.e., all the strong buffering structures are subsets of γ_8^* . Thus, by eliminating γ_8^* , we can get the minimal form of the given reaction

network, $\Gamma' := \Gamma/\gamma_8^*$ with no species and two reactions e_1 and e_2 . The stoichiometric matrix of the minimal form, S' , is given as follows:

$$S = \begin{array}{c} v_1 \\ v_2 \\ v_3 \\ v_4 \end{array} \begin{array}{c} \begin{array}{c} S_{11} \\ \left[\begin{array}{cccc|cc} -1 & -1 & 0 & 0 & 1 & 0 \\ -1 & 0 & 0 & 0 & 0 & 1 \\ 1 & 0 & -1 & 0 & 0 & 0 \\ 0 & 1 & -1 & -1 & 0 & 0 \end{array} \right] \end{array} \\ e_3 \ e_4 \ e_5 \ e_6 \ e_1 \ e_2 \end{array} \longrightarrow S' = \begin{array}{c} [\cdot \ \cdot] \\ e_1 \ e_2 \end{array} \quad (110)$$

Note that the reduced stoichiometric matrix, S' , of size 0×2 , which means that it is a linear map from the two-dimensional vector space to the zero-dimensional one. In the minimal form, the steady-state fluxes is obtained trivially as

$$\begin{bmatrix} r_1 \\ r_2 \end{bmatrix} = \begin{bmatrix} k_1 \\ k_2 \end{bmatrix} = k_1 \mathbf{c}_2^{(1)} + k_2 \mathbf{c}_2^{(2)}, \quad (111)$$

where we picked basis vectors of $\ker S'$ as $\mathbf{c}_2^{(1)} := [1 \ 0]^\top$ and $\mathbf{c}_2^{(2)} := [0 \ 1]^\top$. Using this, we can compute the steady-state fluxes of the original system as

$$\bar{\mathbf{r}} = k_1 \mathbf{c}^{(1)} + k_2 \mathbf{c}^{(2)}, \quad (112)$$

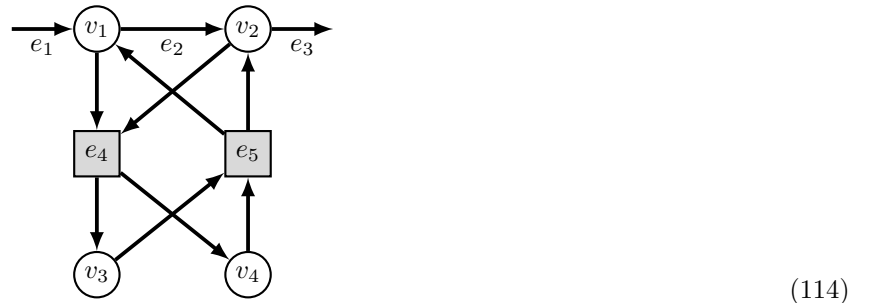
where $\mathbf{c}^{(1)} := [1 \ 0 \ 0 \ 1 \ 0 \ 1]^\top$ and $\mathbf{c}^{(2)} := [0 \ 1 \ 1 \ -1 \ 1 \ -2]^\top$ are the images of $\mathbf{c}_2^{(1)}$ and $\mathbf{c}_2^{(2)}$ via the map $\ker S' \rightarrow \ker S$, and they form a basis of $\ker S$. Since the rate constants of the reactions contained in the strong buffering structure do not affect the steady-state reaction fluxes, $\bar{\mathbf{r}}$ is independent of the rate constants k_3, k_4, k_5 , and k_6 as we can easily check in Eq. (112).

Example 3

Here we describe an example with a conserved charge. We consider a network $\Gamma = (\{v_1, v_2, v_3, v_4\}, \{e_1, e_2, e_3, e_4, e_5\})$ with the following reactions,



The network structure can be drawn as



If we use the mass-action kinetics, the rate equation is written as

$$\frac{d}{dt} \begin{bmatrix} x_1 \\ x_2 \\ x_3 \\ x_4 \end{bmatrix} = \begin{bmatrix} 1 & -1 & 0 & -1 & 1 \\ 0 & 1 & -1 & -1 & 1 \\ 0 & 0 & 0 & 1 & -1 \\ 0 & 0 & 0 & 1 & -1 \end{bmatrix} \begin{bmatrix} r_1 \\ r_2 \\ r_3 \\ r_4 \\ r_5 \end{bmatrix}, \quad \begin{bmatrix} r_1 \\ r_2 \\ r_3 \\ r_4 \\ r_5 \end{bmatrix} = \begin{bmatrix} k_1 \\ k_2 x_1 \\ k_3 x_2 \\ k_4 x_1 x_2 \\ k_5 x_3 x_4 \end{bmatrix}. \quad (115)$$

The kernel and cokernel of the stoichiometric matrix are given by

$$\ker S = \text{span} \{ [1 \ 1 \ 1 \ 0 \ 0]^\top, [0 \ 0 \ 0 \ 1 \ 1]^\top \}, \quad (116)$$

$$\text{coker } S = \text{span} \{ [0 \ 0 \ 1 \ -1]^\top \}. \quad (117)$$

The cokernel is one-dimensional and the system has one conserved charge. To find the steady states, we need to specify the value of the charge as

$$\ell = x_3 - x_4. \quad (118)$$

The steady-state reaction rates and concentrations are

$$\bar{r} = k_1 [1 \ 1 \ 1 \ 0 \ 0]^\top + \frac{k_4 k_1^2}{k_2 k_3} [0 \ 0 \ 0 \ 1 \ 1]^\top, \quad (119)$$

$$\bar{x} = \left[\frac{k_1}{k_2} \ \frac{k_1}{k_3} \ \frac{1}{2} (\ell + \sqrt{\ell^2 + 4K}) \ \frac{1}{2} (-\ell + \sqrt{\ell^2 + 4K}) \right]^\top, \quad (120)$$

where we set $K := k_4 k_1^2 / k_2 k_3$. The buffering structures (except for the network itself) in this example are

$$\gamma_1^* = (\{v_3, v_4\}, \{e_5\}), \quad (121)$$

$$\gamma_2 = (\{v_1, v_3, v_4\}, \{e_2, e_4, e_5\}), \quad (122)$$

$$\gamma_3 = (\{v_2, v_3, v_4\}, \{e_3, e_4, e_5\}). \quad (123)$$

Among these, γ_1^* is a strong buffering structure, which includes a conserved charge $\ell = x_3 - x_4$. Correspondingly, the steady-state reaction rate does not depend on k_5 and ℓ .

The maximal strong buffering structure is γ_1^* . Under the reduction to the minimal form, $\Gamma_{\min} := \Gamma / \gamma_1^*$, the stoichiometric matrix changes as

$$S = \begin{array}{c} v_3 \\ v_4 \\ v_1 \\ v_2 \\ e_5 \end{array} \begin{array}{c} \overset{S_{11}}{\boxed{\begin{array}{ccccc} -1 & 0 & 0 & 0 & 1 \\ -1 & 0 & 0 & 0 & 1 \\ 1 & 1 & -1 & 0 & -1 \\ 1 & 0 & 1 & -1 & -1 \end{array}}} \\ e_1 \ e_2 \ e_3 \ e_4 \end{array} \quad \longrightarrow \quad \begin{array}{c} v_1 \\ v_2 \\ e_1 \ e_2 \ e_3 \ e_4 \end{array} \begin{array}{c} \begin{bmatrix} 1 & -1 & 0 & 0 \\ 0 & 1 & -1 & 0 \end{bmatrix} \end{array} \quad (124)$$

where we have brought the components in γ_1^* to the upper-left part.

METABOLIC PATHWAYS OF *E. COLI*

Here we describe the details of the metabolic pathways of *E. coli* discussed in the main text.

List of reactions

- 1: Glucose + PEP \rightarrow G6P + PYR.
- 2: G6P \rightarrow F6P.
- 3: F6P \rightarrow G6P.
- 4: F6P \rightarrow F16P.
- 5: F16P \rightarrow G3P + DHAP.
- 6: DHAP \rightarrow G3P.
- 7: G3P \rightarrow 3PG.
- 8: 3PG \rightarrow PEP.
- 9: PEP \rightarrow 3PG.
- 10: PEP \rightarrow PYR.

- 11: PYR \rightarrow PEP.
- 12: PYR \rightarrow AcCoA + CO₂.
- 13: G6P \rightarrow 6PG.
- 14: 6PG \rightarrow Ru5P + CO₂.
- 15: Ru5P \rightarrow X5P.
- 16: Ru5P \rightarrow R5P.
- 17: X5P + R5P \rightarrow G3P + S7P.
- 18: G3P + S7P \rightarrow X5P + R5P.
- 19: G3P + S7P \rightarrow F6P + E4P.
- 20: F6P + E4P \rightarrow G3P + S7P.
- 21: X5P + E4P \rightarrow F6P + G3P.
- 22: F6P + G3P \rightarrow X5P + E4P.
- 23: AcCoA + OAA \rightarrow CIT.
- 24: CIT \rightarrow ICT.
- 25: ICT \rightarrow 2-KG + CO₂.
- 26: 2-KG \rightarrow SUC + CO₂.
- 27: SUC \rightarrow FUM.
- 28: FUM \rightarrow MAL.
- 29: MAL \rightarrow OAA.
- 30: OAA \rightarrow MAL.
- 31: PEP + CO₂ \rightarrow OAA.
- 32: OAA \rightarrow PEP + CO₂.
- 33: MAL \rightarrow PYR + CO₂.
- 34: ICT \rightarrow SUC + Glyoxylate.
- 35: Glyoxylate + AcCoA \rightarrow MAL.
- 36: 6PG \rightarrow G3P + PYR.
- 37: AcCoA \rightarrow Acetate.
- 38: PYR \rightarrow Lactate.
- 39: AcCoA \rightarrow Ethanol.
- 40: R5P \rightarrow (output).
- 41: OAA \rightarrow (output).
- 42: CO₂ \rightarrow (output).
- 43: (input) \rightarrow Glucose.
- 44: Acetate \rightarrow (output).
- 45: Lactate \rightarrow (output).
- 46: Ethanol \rightarrow (output).

Buffering structures

We here give the list of buffering structures in the metabolic pathways of *E. coli*. Strong buffering structures are indicated by *.

- $$\begin{aligned} \gamma_1^* &= (\{\text{Glucose}\}, \{1\}), \\ \gamma_2 &= (\{\text{Glucose}, \text{PEP}, \text{G6P}, \text{F6P}, \text{F16P}, \text{DHAP}, \text{G3P}, \text{3PG}, \text{PYR}, \text{6PG}, \text{Ru5P}, \text{X5P}, \text{R5P}, \text{S7P}, \text{E4P}, \text{AcCoA}, \text{OAA}, \\ &\text{CIT}, \text{ICT}, \text{2-KG}, \text{SUC}, \text{FUM}, \text{MAL}, \text{CO}_2, \text{Glyoxylate}, \text{Acetate}, \text{Lactate}, \text{Ethanol}\}, \{1, 2, 3, 4, 5, 6, 7, 8, 9, 10, 11, 12, 13, 14, \\ &15, 16, 17, 18, 19, 20, 21, 22, 23, 24, 25, 26, 27, 28, 29, 30, 31, 32, 33, 34, 35, 36, 37, 38, 39, 40, 41, 42, 44, 45, 46\}), \\ \gamma_3^* &= (\{\text{F16P}\}, \{5\}), \\ \gamma_4^* &= (\{\text{DHAP}\}, \{6\}), \\ \gamma_5 &= (\{\text{G3P}, \text{X5P}, \text{S7P}, \text{E4P}\}, \{7, 17, 18, 19, 20, 21, 22\}), \\ \gamma_6^* &= (\{\text{3PG}\}, \{8\}), \\ \gamma_7 &= (\{\text{Glucose}, \text{PEP}, \text{3PG}, \text{PYR}, \text{AcCoA}, \text{OAA}, \text{CIT}, \text{ICT}, \text{2-KG}, \text{SUC}, \text{FUM}, \text{MAL}, \text{CO}_2, \text{Glyoxylate}, \text{Acetate}, \\ &\text{Lactate}, \text{Ethanol}\}, \{1, 8, 9, 10, 11, 12, 23, 24, 25, 26, 27, 28, 29, 30, 31, 32, 33, 34, 35, 37, 38, 39, 41, 42, 44, 45, 46\}), \\ \gamma_8 &= (\{\text{X5P}, \text{S7P}, \text{E4P}\}, \{17, 18, 19, 20, 21\}), \\ \gamma_9^* &= (\{\text{CIT}\}, \{24\}), \\ \gamma_{10}^* &= (\{\text{2-KG}\}, \{26\}), \end{aligned}$$

$$\begin{aligned}
\gamma_{11}^* &= (\{\text{SUC}\}, \{27\}), \\
\gamma_{12}^* &= (\{\text{FUM}\}, \{28\}), \\
\gamma_{13}^* &= (\{\text{Glyoxylate}\}, \{35\}), \\
\gamma_{14}^* &= (\{\text{X5P}, \text{R5P}, \text{S7P}, \text{E4P}\}, \{17, 18, 19, 20, 21, 40\}), \\
\gamma_{15}^* &= (\{\text{Acetate}\}, \{44\}), \\
\gamma_{16}^* &= (\{\text{Lactate}\}, \{45\}), \\
\gamma_{17}^* &= (\{\text{Ethanol}\}, \{46\}).
\end{aligned}$$

The maximal strong buffering structure is $\bar{\gamma}_s = \gamma_1^* \cup \gamma_3^* \cup \gamma_4^* \cup \gamma_6^* \cup \gamma_9^* \cup \gamma_{10}^* \cup \gamma_{11}^* \cup \gamma_{12}^* \cup \gamma_{13}^* \cup \gamma_{15}^* \cup \gamma_{16}^* \cup \gamma_{17}^*$.

Parameters for the simulation in Figure 2

In the simulation shown in Fig. 2, we employ the mass-action kinetics. In the simulation, the initial concentrations and the reaction rate constants are chosen as: $x_{\text{AcCoA}} = 0.4, x_{\text{Acetate}} = 1.0, x_{\text{CIT}} = 0.2, x_{\text{CO}_2} = 0.6, x_{\text{DHAP}} = 0.2, x_{\text{E4P}} = 0.2, x_{\text{Ethanol}} = 0.5, x_{\text{F16P}} = 0.5, x_{\text{F6P}} = 0.3, x_{\text{FUM}} = 0.1, x_{\text{G3P}} = 1.3, x_{\text{G6P}} = 0.9, x_{\text{Glucose}} = 3.1, x_{\text{Glyoxylate}} = 0.1, x_{\text{ICT}} = 0.1, x_{\text{KG2}} = 0.1, x_{\text{Lactate}} = 0.5, x_{\text{MAL}} = 0.1, x_{\text{OAA}} = 0.1, x_{\text{PEP}} = 0.3, x_{\text{PG3}} = 1.2, x_{\text{PG6}} = 0.3, x_{\text{PYR}} = 0.8, x_{\text{R5P}} = 0.1, x_{\text{Ru5P}} = 0.1, x_{\text{S7P}} = 0.1, x_{\text{SUC}} = 0.1, x_{\text{X5P}} = 4.0$, and $k_1 = 5.0, k_2 = 4.7, k_3 = 7.8, k_4 = 5.7, k_5 = 3.8, k_6 = 9.7, k_7 = 5.0, k_8 = 6.2, k_9 = 3.5, k_{10} = 9.8, k_{11} = 2.5, k_{12} = 6.1, k_{13} = 4.0, k_{14} = 3.8, k_{15} = 7.8, k_{16} = 6.6, k_{17} = 3.8, k_{18} = 5.5, k_{19} = 5.7, k_{20} = 4.7, k_{21} = 8.0, k_{22} = 7.3, k_{23} = 9.2, k_{24} = 1.1, k_{25} = 9.6, k_{26} = 7.4, k_{27} = 7.4, k_{28} = 8.3, k_{29} = 6.2, k_{30} = 6.4, k_{31} = 6.2, k_{32} = 7.9, k_{33} = 9.1, k_{34} = 6.7, k_{35} = 1.6, k_{36} = 9.6, k_{37} = 4.7, k_{38} = 5.1, k_{39} = 7.3, k_{40} = 3.8, k_{41} = 8.4, k_{42} = 9.7, k_{43} = 4.8, k_{44} = 2.0, k_{45} = 8.0, k_{46} = 3.7$. At time $t = 10$, the rate constant k_8 , which is inside the maximum strong buffering structure γ^* , is tripled. At time $t = 30$ the rate constant k_2 , which is outside γ^* , is doubled.

* yuji.hirono@gmail.com

† hphong@kaist.ac.kr

‡ jaekkim@kaist.ac.kr

- [1] T. Okada and A. Mochizuki, Law of localization in chemical reaction networks, *Phys. Rev. Lett.* **117**, 048101 (2016).
- [2] T. Okada and A. Mochizuki, Sensitivity and network topology in chemical reaction systems, *Phys. Rev. E* **96**, 022322 (2017).
- [3] Y. Hirono, T. Okada, H. Miyazaki, and Y. Hidaka, Structural reduction of chemical reaction networks based on topology, *Phys. Rev. Research* **3**, 043123 (2021).